

# Hydrodynamically coupled oscillators

R. TIRON<sup>1</sup>, E. KANSO<sup>1†</sup> AND P. K. NEWTON<sup>1,2</sup>

<sup>1</sup>Department of Aerospace and Mechanical Engineering, University of Southern California,  
Los Angeles, CA 90089, USA

<sup>2</sup>Department of Mathematics, University of Southern California, Los Angeles, CA 90089, USA

(Received 10 August 2010; revised 10 January 2011; accepted 23 February 2011;  
first published online 19 April 2011)

A submerged spring–mass ring is analysed as a simple model for the way in which an underwater swimmer couples its body deformations to the surrounding fluid in order to accomplish locomotion. We adopt an inviscid, incompressible, irrotational assumption for the surrounding fluid and analyse the coupling response to various modes of excitation of the ring configuration. Due to the added mass effect, the surrounding fluid provides an environment which effectively couples the ‘normal modes’ of oscillation of the ring, leading to nonlinear trajectories if the ring is free to accelerate based on the effective forces the oscillations induce. Through a series of examples, we demonstrate various features that the model supports, including the locomotion on curved paths as a result of energy and angular momentum exchange with the surrounding fluid.

**Key words:** flow–structure interactions, nonlinear dynamical systems, swimming/flying

---

## 1. Introduction

The locomotion of many aquatic animals consists of periods of acceleration followed by passive glides, see Videler & Weihs (1982). The coupling between the intrinsic elasticity of the body and the surrounding fluid seems to enhance locomotion during the gliding periods. Indeed, experimental evidence suggests that the elastic properties of the fish body are tuned to hydrodynamic forces; see, for example, Videler (1993), Long & Nipper (1996) and Long *et al.* (1996) for a discussion of the role of body elasticity in undulatory swimming. If one thinks of the underwater swimmer as an elastic body with distributed mass, whose musculature enables it to transmit forces and thus accelerate the surrounding fluid, then a submerged spring–mass model is arguably the simplest prototype that allows a systematic and comprehensive study of the body–fluid coupling to shed light on the main physical mechanisms at play in passive locomotion. The term passive locomotion here refers to locomotion when the system is subject to *only initial excitations* of the body and/or the surrounding fluid. This is in contrast to active locomotion obtained when properly controlling for all time the internal degrees of freedom of the swimming model; see, for example, Kanso *et al.* (2005) and references therein. It is also to be distinguished from passive locomotion in continuously excited external flows such as in the work of Beal *et al.* (2006) on the swimming in vortex wakes.

† Email address for correspondence: kanso@usc.edu

Kanso & Newton (2009) studied the passive locomotion of a rectilinear chain of circular masses connected via linear springs and submerged in a perfect fluid of infinite extent. The masses were constrained to move on a line joining their centres; hence, the locomotion was achieved only in one dimension. In the absence of the fluid, the problem is linear and the normal modes are decoupled, with the eigenfunction corresponding to eigenvalue  $\lambda_1=0$  representing net translation. For the submerged system, the surrounding fluid couples the normal modes and enables such systems to achieve net translation, even when the  $\lambda_1=0$  mode is not initially excited.

In this work, we investigate a class of submerged spring–mass systems that can translate as well as rotate, enabling its geometric centre to move along a two-dimensional path. The system consists of  $n$  circular masses of radii  $a_i, i = 1, \dots, n$ , constrained to move on a circular ring of radius  $R$ . The centres of every two adjacent masses are connected by linear springs of constant stiffness  $k$ . In the limit  $k \rightarrow \infty$ , we refer to the masses as ‘rigidly connected’. The springs are constrained to the ring, such that the elastic forces acting on the cylinders are tangential to it. The system is immersed in an inviscid, incompressible fluid of infinite extent, and the cylinders are considered to be neutrally buoyant. The flow is assumed to be irrotational at all time and at rest at infinity so that we can model and understand the role that the fluid coupling with the elasticity of the body plays in isolation from other effects. The interactions of multiple bodies in irrotational flow are considered in different contexts in the recent works of Grotta Ragazzo (2002, 2003), Burton, Gratus & Tucker (2004), Wang (2004) and Crowdy, Surana & Yick (2007).

We first assess the effect of the fluid–solid coupling on the rotational motion only by fixing the geometric centre of the ring. This can be viewed as the rotational analogue of the rectilinear chain treated in Kanso & Newton (2009). We then consider the case when the geometric centre of the ring is allowed to move freely in the plane. In this case, the main question of interest is the effect of the fluid coupling on the motion of the ring. We show that the coupling of the hydrodynamic effects with the system’s elasticity leads to interesting dynamics not achievable by the hydrodynamically decoupled system nor by the system of rigidly connected masses with no elasticity. For example, we show that for certain initial conditions the spring–mass undergoes a net translational motion, while the hydrodynamically decoupled and the rigidly connected systems remain in place.

## 2. Problem setting

Consider a planar system of  $n$  circular cylinders  $B_i$  of radii  $a_i, i = 1, \dots, n$ , constrained to move on a massless circular ring of radius  $R$ . The geometric centre  $O$  of the ring is free to move in the plane of motion of the cylinders, see figure 1. The centres of every two adjacent masses are connected by linear springs of constant stiffness  $k$ . The springs are constrained to the ring such that the elastic forces acting on the cylinders are tangential to the ring. The spring–mass system is immersed in an inviscid, incompressible fluid of infinite extent which is assumed to remain irrotational at all time and at rest at infinity. The cylinders are considered to be neutrally buoyant, that is to say, the cylinders and the fluid have the same uniform density  $\rho$ .

Let  $\{\mathbf{e}_{1,2,3}\}$  be an orthonormal inertial frame where  $\{\mathbf{e}_{1,2}\}$  spans the plane of motion. The configuration of the system can be described by the position vectors

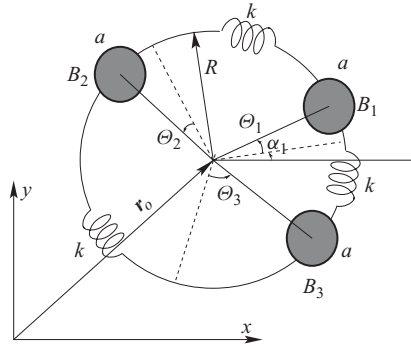


FIGURE 1. Spring–mass system in ring formation for a system comprised of three cylinders. The three cylinders of radii  $a$  are constrained to move on a ring of radius  $R$  and are connected via linear springs of constant  $k$ , such that the elastic forces act tangentially to the ring. The angles at equilibrium are denoted by  $\alpha_i$ , whereas the angular deformations by  $\Theta_i$ ,  $i = 1, \dots, 3$ .

$\mathbf{r}_i = x_i \mathbf{e}_1 + y_i \mathbf{e}_2$  of the cylinders' centres subject to the  $n$  constraints  $(x_i - x_0)^2 + (y_i - y_0)^2 = R^2$ , where  $(x_0, y_0)$  denote the coordinates of the geometric centre of the ring. Equivalently, the system's configuration can be described in terms of  $\mathbf{r}_0 = x_0 \mathbf{e}_1 + y_0 \mathbf{e}_2$  and the positions  $(\mathbf{r}_i - \mathbf{r}_0)$  of the cylinders relative to the ring centre, the latter being parameterized by the angular placement of the cylinders on the ring. When the system is in equilibrium, that is to say, the springs are undeformed, the corresponding placement of the cylinders along the ring can be described by the angles  $\alpha_i$  measured counter-clockwise from the  $x$ -axis. As the springs deform, the angular coordinates of the cylinders, measured from the undeformed configuration, are denoted by  $\Theta_i$ . Clearly, one has

$$x_i = x_0 + R \cos(\alpha_i + \Theta_i), \quad y_i = y_0 + R \sin(\alpha_i + \Theta_i). \tag{2.1}$$

It is convenient to introduce the  $2n$ -dimensional position vector  $\mathbf{X} \equiv \{x_1, y_1, \dots, x_n, y_n\}^T$ , where  $()^T$  denotes the transpose, and the  $n$ -dimensional angular position vector  $\boldsymbol{\Theta} = (\Theta_1, \Theta_2, \dots, \Theta_n)^T$ . If the ring's centre is fixed, say at the origin of the inertial frame  $(x_0, y_0) \equiv (0, 0)$ , the configuration of the system can be determined by the  $n$  variables  $\Theta_i$ . Then using the constraint equations (2.1) one can readily verify that the reduced (that is to say, unconstrained) velocity vector  $\dot{\boldsymbol{\Theta}} := d\boldsymbol{\Theta}/dt$ , with  $t$  being time, is related to the velocity vector  $\dot{\mathbf{X}}$  via the transformation

$$\dot{\mathbf{X}} = \mathbf{R}_{fixed} \dot{\boldsymbol{\Theta}}, \tag{2.2}$$

where the  $2n \times n$  matrix  $\mathbf{R}_{fixed}$  is given by

$$\mathbf{R}_{fixed} = \begin{pmatrix} -R \sin(\Theta_1 + \alpha_1) & 0 & \dots & 0 \\ R \cos(\Theta_1 + \alpha_1) & 0 & \dots & 0 \\ 0 & -R \sin(\Theta_2 + \alpha_2) & \dots & 0 \\ 0 & R \cos(\Theta_2 + \alpha_2) & \dots & 0 \\ \vdots & \vdots & \vdots & \vdots \\ 0 & 0 & \dots & -R \sin(\Theta_n + \alpha_n) \\ 0 & 0 & \dots & R \cos(\Theta_n + \alpha_n) \end{pmatrix}. \tag{2.3}$$

If the ring is free to move in the plane, its configuration can be described by the reduced  $(n + 2)$ -dimensional position vector  $\boldsymbol{\zeta} \equiv \{x_0, y_0, \Theta_1, \Theta_2, \dots, \Theta_n\}^T$ . Similarly to (2.2), one can readily verify that

$$\dot{\boldsymbol{X}} = \mathbf{R}_{free} \dot{\boldsymbol{\zeta}}, \tag{2.4}$$

where the  $2n \times (n + 2)$  matrix  $\mathbf{R}_{free}$  is given by

$$\mathbf{R}_{free} = \left( \begin{array}{c|c} I_{2 \times 2} & \\ \vdots & \vdots \mathbf{R}_{fixed} \\ I_{2 \times 2} & \end{array} \right), \tag{2.5}$$

where  $I_{2 \times 2}$  is the  $2 \times 2$  identity matrix.

### 3. Equations of motion

We derive the equations of motion for the fluid–mass system using Hamilton’s least action principle for which the Lagrangian function is given by

$$\mathcal{L} = T - U \tag{3.1}$$

where  $T = T_B + T_F$  denotes the kinetic energy of the fluid–mass system, whereas  $U$  denotes the potential energy stored in the springs. The potential energy  $U$  stored in the springs can be written in matrix form as

$$U = \frac{1}{2} \boldsymbol{\Theta}^T \mathbf{K} \boldsymbol{\Theta}, \tag{3.2}$$

where the stiffness matrix is given by

$$\mathbf{K} = k \begin{pmatrix} 2 & -1 & 0 & \cdots & 0 & -1 \\ -1 & 2 & -1 & \cdots & 0 & 0 \\ \vdots & \vdots & \vdots & \ddots & \vdots & \vdots \\ 0 & 0 & 0 & \cdots & 2 & -1 \\ -1 & 0 & 0 & \cdots & -1 & 2 \end{pmatrix} \quad \text{or } \mathbf{K} = k \begin{pmatrix} 2 & -2 \\ -2 & 2 \end{pmatrix} \quad \text{if } n = 2. \tag{3.3}$$

The kinetic energy  $T_B$  of the  $n$  cylinders is given by

$$T_B = \frac{1}{2} \dot{\boldsymbol{X}}^T \mathbf{M}_{cyl} \dot{\boldsymbol{X}}, \tag{3.4}$$

where  $\mathbf{M}_{cyl}$  is a  $2n \times 2n$  diagonal mass matrix with block entries  $\rho \pi a_i^2 I_{2 \times 2}$ . In potential flow, the kinetic energy of the fluid  $T_F$  can be written, using standard vector identities and techniques (see for example Kanso *et al.* 2005 and Nair & Kanso 2007), as a function of the positions  $\boldsymbol{X}$  and velocities  $\dot{\boldsymbol{X}}$  of the submerged bodies,

$$T_F = \frac{1}{2} \dot{\boldsymbol{X}}^T \mathbf{M}_{added} \dot{\boldsymbol{X}}. \tag{3.5}$$

The added mass matrix  $\mathbf{M}_{added}$  is a  $2n \times 2n$  symmetric matrix that accounts for the presence of the fluid. Differently said, in potential flow, the hydrodynamic forces

acting on the surfaces of the accelerating bodies can be completely accounted for by ‘adding mass’ to the submerged bodies (see Brennen 1982 for a comprehensive review). The entries of the added mass matrix  $\mathbf{M}_{added}$  depend not only on the shape of the submerged bodies, here considered to be circular cylinders, but also on their position relative to each other  $(x_i - x_j, y_i - y_j)$ ,  $i \neq j$  and  $i, j = 1, \dots, n$ . In the case considered here where the  $n$  masses are constrained to move along the ring, these relative positions can be parameterized by  $\Theta$ . Approximate expressions for  $\mathbf{M}_{added}(\Theta)$  are derived in §4.

When the ring’s centre is fixed, one finds, by adding (3.4) and (3.5) and substituting (2.2) into the resulting expression, that the total kinetic energy  $T = T_B + T_F$  of the fluid–mass system can be written as a function of  $\Theta$  and  $\dot{\Theta}$  only:

$$T = \frac{1}{2} \dot{\Theta}^T \mathbf{M}_{fixed} \dot{\Theta}, \quad \mathbf{M}_{fixed} = \mathbf{R}_{fixed}^T (\mathbf{M}_{cyl} + \mathbf{M}_{added}(\Theta)) \mathbf{R}_{fixed}, \tag{3.6}$$

where  $\mathbf{M}_{fixed}$  is an  $n \times n$  mass matrix function of  $\Theta$  only. In the case when the ring is free to move in the plane, one finds, by virtue of (2.4), that the total kinetic energy of the fluid–mass system takes the form

$$T = \frac{1}{2} \dot{\xi}^T \mathbf{M}_{free} \dot{\xi}, \quad \mathbf{M}_{free} = \mathbf{R}_{free}^T (\mathbf{M}_{cyl} + \mathbf{M}_{added}(\Theta)) \mathbf{R}_{free}, \tag{3.7}$$

where  $\mathbf{M}_{free}$  is an  $(n + 2) \times (n + 2)$  mass matrix also the function of  $\Theta$  only. It is worth noting that the mass matrix  $\mathbf{R}_{fixed}^T \mathbf{M}_{cyl} \mathbf{R}_{fixed}$  in (3.6) accounting for the inertia of the cylinders only is a diagonal matrix with constant entries  $\rho \pi a_i^2$ , which implies that the dynamics of this fixed ring system in the absence of the fluid is linear. This is in contrast to the case when the centre of the ring is free to move in the plane. Indeed, in (3.7), the mass matrix  $\mathbf{R}_{free}^T \mathbf{M}_{cyl} \mathbf{R}_{free}$  accounting for the inertia of the cylinders only is no longer a diagonal matrix and depends nonlinearly on the configuration vector  $\Theta$ . Thus, even in the absence of the fluid, the dynamics of the spring–mass system on the ring is nonlinear.

The Lagrangian function  $\mathcal{L}$  of the fixed ring can then be rewritten, using (3.2) and (3.6), as a function of  $\Theta$  and  $\dot{\Theta}$  only:

$$\mathcal{L}(\Theta, \dot{\Theta}) = \frac{1}{2} \dot{\Theta}^T \mathbf{M}_{fixed}(\Theta) \dot{\Theta} - \frac{1}{2} \Theta^T \mathbf{K} \Theta. \tag{3.8}$$

In the absence of external forces and moments acting on the fluid–mass system, the equations of motion are given by the Euler–Lagrange equations

$$\frac{d}{dt} \left( \frac{\partial \mathcal{L}}{\partial \dot{\Theta}} \right) - \frac{\partial \mathcal{L}}{\partial \Theta} = 0. \tag{3.9}$$

This class of problems is energy-preserving, and the total energy  $E = \frac{1}{2} \dot{\Theta}^T \mathbf{M}_{fixed} \dot{\Theta} + \frac{1}{2} \Theta^T \mathbf{K} \Theta$  is conserved. It also admits a momentum integral of motion, namely the momentum of the fluid–mass system associated with a rigid or net rotation of the system is conserved (as verified below via examples). In other words, if  $\Theta = (\sum_i \Theta_i) / n$  is the net rigid rotation of the ring, the total angular momentum  $h = \partial \mathcal{L} / \partial \dot{\Theta}$  is conserved.

In the case when the ring is free to move in the plane, the Lagrangian function can be expressed in terms of  $\xi$  and  $\dot{\xi}$  only:

$$\mathcal{L}(\xi, \dot{\xi}) = \frac{1}{2} \dot{\xi}^T \mathbf{M}_{free}(\Theta) \dot{\xi} - \frac{1}{2} \Theta^T \mathbf{K} \Theta. \tag{3.10}$$

Similarly to the fixed case, one can derive the equations of motion of the system in terms of the  $n + 2$  variables  $\zeta$ . Since the entries of the  $(n + 2) \times (n + 2)$  mass matrix  $\mathbf{M}_{free}$  depend exclusively on  $\Theta$ , the coordinates of the geometric centre  $x_0, y_0$  are the ignorable coordinates of the Lagrangian, and the associated linear momenta  $p_x = \partial \mathcal{L} / \partial \dot{x}_0$  and  $p_y = \partial \mathcal{L} / \partial \dot{y}_0$  are conserved. These two symmetries reflect the fact that the system’s dynamics is invariant to rigid translations of the ring’s centre. As in the case of the fixed ring, one has two additional symmetries due to invariance of the system to rigid rotations and due to re-parameterization of time. The last symmetry is associated with conservation of the system’s total energy  $E = T + U$ , while the rotational symmetry is associated with conservation of the system’s total angular momentum  $h = \partial \mathcal{L} / \partial \dot{\Theta} + x_0(\partial \mathcal{L} / \partial \dot{y}_0) - y_0(\partial \mathcal{L} / \partial \dot{x}_0)$ .

When the spring stiffness is infinite, that is to say, the cylinders are rigidly connected on the ring, the system has no elastic energy  $U = 0$  and the variables  $\Theta_i$  are equal. The configuration of the free ring can then be determined by the variables  $x_0, y_0$  and  $\Theta$  only. The resulting Euler–Lagrange equations  $\dot{p}_x = 0, \dot{p}_y = 0$  and  $\dot{h} = 0$  which reflect conservation of total linear and angular momenta of the fluid–mass system are identical to the well-known Kirchhoff’s equations for a submerged rigid body; see for example Kanso *et al.* (2005) and Lamb (1932) for more details.

**4. Approximate added mass matrices**

We obtain approximate expressions for the added mass matrix  $\mathbf{M}_{added}$  in (3.5) by assuming that the distances between the cylinders are much bigger than their radii. To fix ideas, we first construct the approximate added mass matrix for the case of two cylinders, of radii  $a_1$  and  $a_2$ , free to move in the plane, that is to say, not constrained to the ring. The derivation, which we omit here for the sake of brevity, follows closely the discussion in Nair & Kanso (2007) for the case of two cylinders free to move along the line connecting their centres. The main difference is that here we let each of the cylinders move with unit speed in the  $\mathbf{e}_1$ - and  $\mathbf{e}_2$ -directions, respectively, while the other cylinder is fixed. We compute approximate expressions for Kirchhoff’s potentials caused by each of these motions. We then calculate the entries of the added mass matrix as integral functions of these Kirchhoff’s potentials – the interested reader is referred to Nair & Kanso (2007) and Lamb (1932) for more details. To this end, one obtains

$$\mathbf{M}_{added} \approx \begin{pmatrix} \rho \pi a_1^2 I_{2 \times 2} & (\mathbf{M}_{added})_{12} \\ (\mathbf{M}_{added})_{12} & \rho \pi a_2^2 I_{2 \times 2} \end{pmatrix}, \tag{4.1}$$

where  $I_{2 \times 2}$  is the  $2 \times 2$  identity matrix and the off-diagonal block matrix is given by

$$(\mathbf{M}_{added})_{12} = -\rho \pi \frac{2a_1^2 a_2^2}{r_{12}^2} \begin{pmatrix} \cos 2\alpha_{12} & \sin 2\alpha_{12} \\ \sin 2\alpha_{12} & -\cos 2\alpha_{12} \end{pmatrix}. \tag{4.2}$$

Here,  $r_{12}^2 = (x_2 - x_1)^2 + (y_2 - y_1)^2$  is the square of the distance between the two cylinders and  $\alpha_{12}$  is the angle measured from the  $\mathbf{e}_1$ -direction to the line connecting the centres of the two cylinders.

We generalize these approximate expressions to the case of  $n$  submerged cylinders by assuming that every two cylinders affect each other as if they were the only two

in the fluid domain. Namely we write

$$\mathbf{M}_{added} \approx \begin{pmatrix} \rho\pi a_1^2 I_{2 \times 2} & (\mathbf{M}_{added})_{12} & \cdots & (\mathbf{M}_{added})_{1n} \\ (\mathbf{M}_{added})_{12} & \rho\pi a_2^2 I_{2 \times 2} & \cdots & (\mathbf{M}_{added})_{2n} \\ \vdots & & \ddots & \\ (\mathbf{M}_{added})_{1n} & (\mathbf{M}_{added})_{2n} & \cdots & \rho\pi a_n^2 I_{2 \times 2} \end{pmatrix}, \tag{4.3}$$

where  $(\mathbf{M}_{added})_{ij}$  for  $i \neq j$  is given as in (4.2).

When the centres of the cylinders are constrained to the ring, the components of  $\mathbf{M}_{added}$  can readily be expressed in terms of the configuration vector  $\Theta$  by noting that

$$\left. \begin{aligned} 2\alpha_{ij} &= \Theta_i + \Theta_j + \alpha_i + \alpha_j - \pi, \\ r_{ij}^2 &= 2R^2(1 - \cos[\Theta_i - \Theta_j + \alpha_i - \alpha_j]). \end{aligned} \right\} \tag{4.4}$$

In order to highlight that the resulting expressions for the added mass are valid only when the distances between the cylinders are much bigger than their radii, it is useful to introduce a small scaling parameter  $\epsilon$  of the same order as  $a/R \ll 1$ , where  $a$  is the maximum of the cylinders radii and  $R$ , the radius of the ring, characterizes the separation between the cylinders. We then define the scaled non-dimensional parameters  $\tilde{a}_i$  and  $\tilde{m}$  and scaled variables  $\tilde{\Theta}_i$ :

$$\epsilon \tilde{a}_i = \frac{a_i}{R}, \quad \tilde{m}_{ij} = \frac{m_{ij}}{\rho\pi a^2}, \quad \epsilon \tilde{\Theta}_i = \Theta_i, \tag{4.5}$$

where  $m_{ij}$  stands for any entry of the added mass matrix  $\mathbf{M}_{added}$ . For consistency with the non-dimensionalization in (4.5),  $x_0$  and  $y_0$  are scaled as  $\epsilon \tilde{x}_0 = x_0/R$  and  $\epsilon \tilde{y}_0 = y_0/R$ . Time is scaled as  $\tilde{t} = \omega_n t$  where  $\omega_n$  is a ‘nominal’ frequency defined as  $\omega_n = \sqrt{k_n/(\rho\pi a^2)}$  with  $k_n$  being a constant spring stiffness whose value is of the same order of  $k$ . The spring stiffness is non-dimensionalized using  $\tilde{k} = k/\rho\pi a^2 \omega_n^2$ . Note that the value of  $k_n$  can be set to be equal to  $k$  in which case  $\tilde{k} = 1$  or alternatively, as done throughout this paper,  $k_n$  can be chosen such that  $\omega_n = 1$  and the dimensionless spring stiffness  $\tilde{k}$  remains a free parameter. Now, upon substituting (4.4) and (4.5) into (4.3), one gets the entries of the non-dimensional added mass matrix when the cylinders are constrained to move on the ring, namely

$$(\mathbf{M}_{added})_{ii} = m_i^\theta I_{2 \times 2}, \quad m_i^\theta = \frac{a_i^2}{a^2}, \tag{4.6}$$

and, for  $i \neq j$ ,

$$(\mathbf{M}_{added})_{ij} = -\epsilon^2 m_{ij}^\theta \begin{pmatrix} \cos[\epsilon(\Theta_i + \Theta_j) + \alpha_i + \alpha_j] & \sin[\epsilon(\Theta_i + \Theta_j) + \alpha_i + \alpha_j] \\ \sin[\epsilon(\Theta_i + \Theta_j) + \alpha_i + \alpha_j] & -\cos[\epsilon(\Theta_i + \Theta_j) + \alpha_i + \alpha_j] \end{pmatrix}, \tag{4.7}$$

where

$$m_{ij}^\theta = -\frac{a_i^2 a_j^2}{a^2 (1 - \cos[\epsilon(\Theta_i - \Theta_j) + \alpha_i - \alpha_j])}. \tag{4.8}$$



Note that in (4.6)–(4.8), we dropped the tilde notation, considering all variables are non-dimensional. When adding the dimensionless mass of the cylinders to the added mass matrix, the non-dimensional mass matrix  $\mathbf{M}_{fixed} = \mathbf{R}_{fixed}^T (\mathbf{M}_{cyl} + \mathbf{M}_{added}) \mathbf{R}_{fixed}$  in (3.6) takes a particularly simple form with diagonal entries equal to  $2m_i^\theta$  and off-diagonal entries equal to  $\epsilon^2 m_{ij}^\theta$ .

### 5. Hydrodynamically decoupled dynamics

When the off-diagonal entries of the added mass matrix  $\mathbf{M}_{added}$  in (4.3) are zero ( $m_{ij}^\theta = 0, i \neq j$ ), the diagonal entries correspond to the added mass of each cylinder as if it were alone in the fluid domain without accounting for the presence of the other cylinders. To this end, the submerged cylinders are said to be hydrodynamically decoupled.

For the case when the ring’s centre is fixed and  $m_{ij}^\theta = 0, i \neq j$  (which is equivalent to setting  $\epsilon = 0$ ), one can readily verify that the mass matrix  $\mathbf{M}_{fixed}$ , relabelled as  $\mathbf{M}_{decoupled}$ , is diagonal with constant entries equal to  $2a_i^2/a^2$ . The dynamics is thus linear and the equations of motion (3.9) take the form

$$\mathbf{M}_{decoupled} \ddot{\Theta} + \mathbf{K}\Theta = 0. \tag{5.1}$$

It is worth emphasizing here that this result is true only for the fixed ring. The dynamics of the free ring is nonlinear even when hydrodynamically decoupled ( $m_{ij}^\theta = 0, i \neq j$ ). The nonlinearity stems from the geometric constraints in (2.1) and (2.4) which makes the mass matrix  $\mathbf{M}_{free}$  in (3.7) depend nonlinearly on  $\Theta$  even when the mass matrices  $\mathbf{M}_{cyl}$  and  $\mathbf{M}_{added}$  are diagonal.

Solutions of (5.1) can be expressed in terms of the system’s normal modes corresponding to the eigenvalues  $\lambda_i$  and eigenvectors  $\mathbf{v}^{(i)}$  of the matrix  $\mathbf{M}_{decoupled}^{-1} \mathbf{K}$ . Indeed, one has  $\mathbf{M}_{decoupled}^{-1} \mathbf{K} = \mathbf{V} \mathbf{\Lambda} \mathbf{V}^{-1}$ , where  $\mathbf{\Lambda}$  is a positive diagonal matrix whose entries correspond to the eigenvalues of  $\mathbf{M}_{decoupled}^{-1} \mathbf{K}$ , while the columns of  $\mathbf{V}$  correspond to its eigenvectors. Now, letting  $\mathbf{\Gamma} = \mathbf{V}^{-1} \Theta$ , (5.1) can be rewritten in the convenient form

$$\ddot{\mathbf{\Gamma}} + \mathbf{\Lambda} \mathbf{\Gamma} = 0. \tag{5.2}$$

The solution of (5.2) is given by the normal modes

$$\left. \begin{aligned} \Gamma_1(t) &= \Gamma_1(0) + \dot{\Gamma}_1(0)t \\ \Gamma_i(t) &= \Gamma_i(0) \cos(\omega_i t) + \frac{\dot{\Gamma}_i(0)}{\omega_i} \sin(\omega_i t), \quad i = 2, \dots, n. \end{aligned} \right\} \tag{5.3}$$

Here,  $\Gamma_1(t)$  represents the rigid rotation of the ring corresponding to the zero eigenvalue  $\lambda_1 = 0$  (guaranteed by the fact that all the rows of  $\mathbf{K}$  sum to zero) and its associated eigenvector  $\mathbf{v}^{(1)} = \{1/\sqrt{n}, \dots, 1/\sqrt{n}\}^T$  while  $\Gamma_i$  (for  $i \geq 2$ ) are purely oscillation modes with oscillation frequencies  $\omega_i = \sqrt{\lambda_i}$ . Note that the rigid rotation  $\Theta$  defined in §3 is equal to  $\Gamma_1$  modulo a multiplication constant,  $\Theta = \Gamma_1/\sqrt{n}$ , which is inconsequential to the dynamics.

In the case of identical cylinders (equal radii  $a_i = a$ ), the diagonal mass matrix  $\mathbf{M}_{decoupled}$  has equal entries  $m$ . The matrix  $\mathbf{M}_{decoupled}^{-1} \mathbf{K}$  is symmetric and  $\mathbf{V}$  is orthogonal ( $\mathbf{V}^{-1} = \mathbf{V}^T$ ) which allows one to find closed form expressions for the eigenvalues and eigenvectors of  $\mathbf{M}_{decoupled}^{-1} \mathbf{K}$ . Namely, one has

$$\lambda_i = \frac{2k}{m} \left( 1 - \cos \frac{2\pi(i-1)}{n} \right), \quad m = 2, \quad i = 1, \dots, n, \tag{5.4}$$



and  $(\sqrt{n}/\sqrt{2})V$  is equal to

$$\begin{pmatrix} \frac{1}{\sqrt{2}} & 1 & 1 & \cdots & -\frac{1}{\sqrt{2}} & \cdots & 0 & 0 \\ \frac{1}{\sqrt{2}} & \cos \frac{2\pi}{n} & \cos \frac{4\pi}{n} & \cdots & \frac{1}{\sqrt{2}} & \cdots & \sin \frac{4\pi}{n} & \sin \frac{2\pi}{n} \\ \vdots & \vdots & \vdots & & \vdots & & \vdots & \vdots \\ \frac{1}{\sqrt{2}} & \cos \frac{2\pi(n-2)}{n} & \cos \frac{4\pi(n-2)}{n} & \cdots & -\frac{1}{\sqrt{2}} & \cdots & \sin \frac{4\pi(n-2)}{n} & \sin \frac{2\pi(n-2)}{n} \\ \frac{1}{\sqrt{2}} & \cos \frac{2\pi(n-1)}{n} & \cos \frac{4\pi(n-1)}{n} & \cdots & \frac{1}{\sqrt{2}} & \cdots & \sin \frac{4(n-1)\pi}{n} & \sin \frac{2\pi(n-1)}{n} \end{pmatrix} \quad (5.5)$$

for  $n$  even, whereas for  $n$  odd the middle column is absent.

When  $\epsilon \neq 0$ , the hydrodynamic coupling between the masses causes the normal modes to couple in general yielding interesting dynamics not achievable when  $\epsilon = 0$  as detailed in §6.

### 6. Dynamic response of the submerged spring–mass system

In this section, we analyse the dynamics of the submerged spring–mass system. We particularly highlight the system’s dynamics in comparison to two limiting cases: (i) the case  $m_{ij}^\theta = 0, i \neq j$ , which reflects the system’s response when it is hydrodynamically decoupled and (ii) the case of infinite spring stiffness  $k$  which reflects the submerged rigid-body dynamics of the free ring with no elasticity. Note that in order to compare the motion of the deformable spring–mass system to the motion of the ‘locked’ system (infinite  $k$ ), we have to translate the initial conditions given for the deformable system in terms of  $\boldsymbol{\zeta}(0) \equiv \{x_o(0), y_o(0), \Theta_i(0)\}^T$  and  $\dot{\boldsymbol{\zeta}}(0) \equiv \{\dot{x}_o(0), \dot{y}_o(0), \dot{\Theta}_i(0)\}^T$  to the rigid system where the variables  $\Theta_i$  are equal. This is done by computing the total linear and angular momenta imparted by the initial conditions  $\boldsymbol{\zeta}(0)$  and  $\dot{\boldsymbol{\zeta}}(0)$  to the spring–mass system and using these momenta to compute the initial linear and angular velocities of the corresponding ‘locked’ rigid system. In order words, in comparing the trajectories of the deformable and rigid systems, we ensure that the initial total momenta in both cases are identical.

#### 6.1. Fixed ring

For concreteness, we consider the case of three masses of equal radii  $a$  that are uniformly spaced on the ring in the undeformed equilibrium configuration. The solution of the hydrodynamically decoupled system is expressed analytically in terms of its normal modes  $\Gamma_1(t), \Gamma_2(t), \Gamma_3(t)$  and their associated frequencies  $\omega_1 = 0, \omega_2 = \omega_3 = \sqrt{3k/m}$ . Note that the solutions of the decoupled problem do not depend on the equilibrium spacing between the cylinders. To highlight the effect of the hydrodynamic coupling on the system’s response, we project the dynamics of the coupled system on the normal modes of the decoupled one. That is, we use the coordinate transformation  $\boldsymbol{\Gamma} = V^T \boldsymbol{\Theta}$  which can be written in component form as

$$\Gamma_1 = \frac{1}{\sqrt{3}}(\Theta_1 + \Theta_2 + \Theta_3), \quad \Gamma_2 = \frac{1}{\sqrt{6}}(2\Theta_1 - \Theta_2 - \Theta_3), \quad \Gamma_3 = \frac{1}{\sqrt{2}}(\Theta_2 - \Theta_3). \quad (6.1)$$

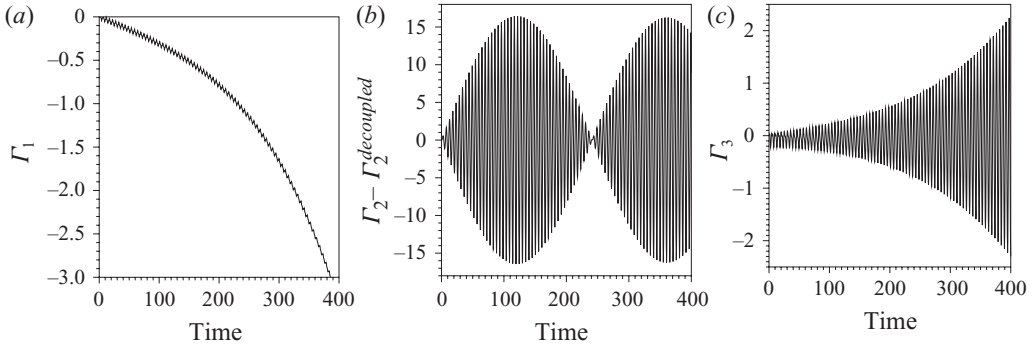


FIGURE 2. Submerged three-mass system on a fixed ring. Starting with zero angular velocity  $\dot{\Gamma}_1(0)=0$ , the submerged system is capable of achieving net rotation by initially exciting impulsively the oscillatory mode  $\Gamma_2$ . The initial conditions are  $\Gamma_1(0)=\Gamma_2(0)=\Gamma_3(0)=0$ ,  $\dot{\Gamma}_1(0)=\dot{\Gamma}_3(0)=0$  and  $\dot{\Gamma}_2(0)=10$ . The parameters are set to  $k=1$ ,  $\epsilon=0.1$ ,  $a=3$  and the cylinders are equally spaced at equilibrium. The integration time is 400.

When expressed in terms of the  $\mathbf{\Gamma}$  coordinates, the stiffness matrix  $V^T \mathbf{K} V$  is a diagonal matrix with entries  $0, 3k$  and  $3k$ , respectively, whereas the symmetric mass matrix  $V^T \mathbf{M}_{fixed}(\mathbf{\Gamma}) V$  (which includes the mass plus added mass effect) takes the form

$$\begin{pmatrix} m + \frac{2\epsilon^2}{3}(m_{12} + m_{13} + m_{23}) & \frac{\epsilon^2}{3\sqrt{2}}(m_{12} + m_{13} - 2m_{23}) & \frac{\epsilon^2}{\sqrt{6}}(m_{12} - m_{13}) \\ \frac{\epsilon^2}{3\sqrt{2}}(m_{12} + m_{13} - 2m_{23}) & m + \frac{\epsilon^2}{3}(m_{23} - 2m_{12} - 2m_{13}) & \frac{\epsilon^2}{\sqrt{3}}(m_{12} - m_{13}) \\ \frac{\epsilon^2}{\sqrt{6}}(m_{12} - m_{13}) & \frac{\epsilon^2}{\sqrt{3}}(m_{12} - m_{13}) & m - \epsilon^2 m_{23} \end{pmatrix}. \tag{6.2}$$

The scaled total angular momentum  $h = \partial L / \partial \dot{\Gamma}_1$  of the fluid–solid system is a conserved quantity and takes the form

$$h = \left[ m + \frac{2\epsilon^2}{3}(m_{12} + m_{13} + m_{23}) \right] \dot{\Gamma}_1 + \frac{\epsilon^3}{3\sqrt{2}}(m_{12} + m_{13} - 2m_{23}) \dot{\Gamma}_2 + \frac{\epsilon^2}{\sqrt{6}}(m_{12} - m_{13}) \dot{\Gamma}_3. \tag{6.3}$$

By proper initial excitation of the oscillation modes only, the submerged spring–mass system can undergo a net rotation due to the hydrodynamic coupling. Obviously, such oscillation-induced rotations cannot be achieved in the context of the hydrodynamically decoupled system. Figure 2 shows the response of the spring–mass system relative to the response of the decoupled system (5.3) subject to zero rotational velocity  $\dot{\Gamma}_1(0)=0$  at  $t=0$  and an initial impulsive excitation to the oscillatory mode  $\Gamma_2$ . Clearly, a net rotation is achieved due to the coupling of the masses via the ambient fluid. Remarkably, the total angular momentum  $h$  of the fluid–solid system given in (6.3) is zero in this case, see figure 3. However, the term  $h_{rotation} = [m + (2\epsilon^2/3)(m_{12} + m_{13} + m_{23})] \dot{\Gamma}_1$  associated with  $\dot{\Gamma}_1$  starts to oscillate for  $t > 0$ , see figure 3(a), while exhibiting a net drift over these oscillations as evident in figure 3(b).

This oscillation-induced rotation can be enhanced by modifying the equilibrium configuration (results not shown here), that is to say, the location of the masses on

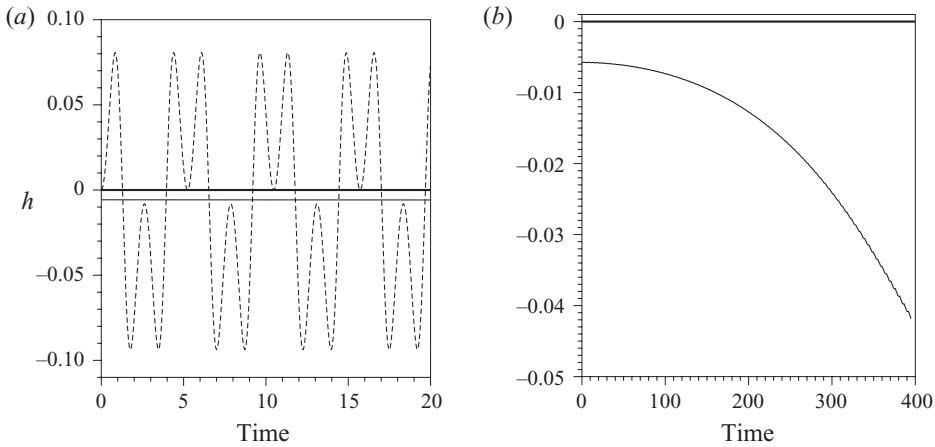


FIGURE 3. Submerged three-mass system on a fixed ring. Angular momentum for the case shown in figure 2. (a) Thick line – the total (fluid + body) angular momentum, dashed line – the angular momentum associated with rotation  $h_{rotation} = [m + (2\epsilon^2/3)(m_{12}^\theta + m_{13}^\theta + m_{23}^\theta)]\dot{\Gamma}_1$ , and thin line – the average of the angular momentum associated with  $h_{rotation}$  obtained by taking  $\bar{h}_{rotation}(t) = (1/T) \int_t^{t+T} h_{rotation}(s) ds$ , where  $T = 5.2$  s gives a scale of the oscillations shown by the dashed line. (b) Long-time behaviour of the average  $\bar{h}_{rotation}(t) = (1/T) \int_t^{t+T} h_{rotation}(s) ds$ .

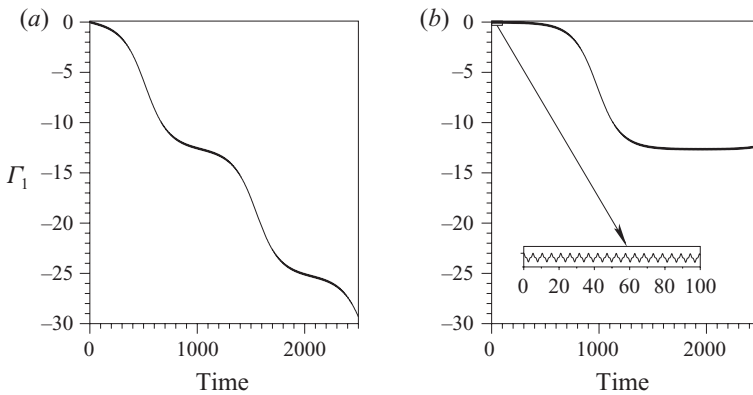


FIGURE 4. Submerged three-mass system on a fixed ring. Long-time response projected on the rigid rotation normal mode (a) for the case in figure 2 and (b) for the same system but starting from rest ( $\dot{\Gamma}_1(0) = \dot{\Gamma}_2(0) = \dot{\Gamma}_3(0) = 0$ ) with initial conditions in deformation  $\Gamma_1(0) = \Gamma_3(0) = 0$  and  $\Gamma_2(0)$  chosen such that the energy  $E = U(0)$  is the same as in (a). The integration time in both cases is 2500. The long-time response of the system depends on the type of initial excitation. When the initial excitation is given in terms of deformation angle only, the net rotation remains bounded.

the ring at equilibrium. This is in contrast to the behaviour of the hydrodynamically decoupled system which does not depend on how the cylinders are placed on the ring at equilibrium. We also note that the hydrodynamically coupled system exhibits distinct long-term dynamics depending on whether the initial excitation is given in terms of oscillation velocity or deformation, see figure 4, whereas for the decoupled system, the two initial conditions lead only to a phase difference in the system's response.

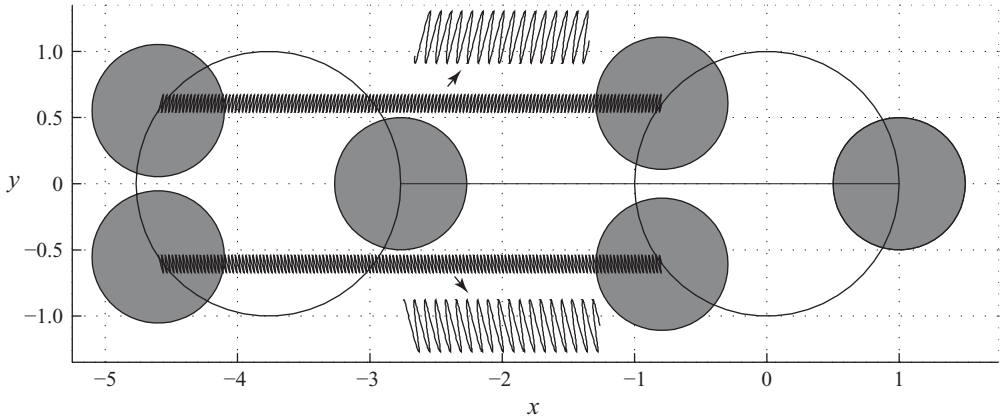


FIGURE 5. Submerged three-mass system on a free ring. The hydrodynamically coupled system is able to achieve net locomotion while, for the same initial conditions, the hydrodynamically decoupled and rigidly locked systems remain in place. Configurations of the system at  $t=0$  and  $t=100$  are superimposed on the trajectory of the ring's centre. The non-zero initial conditions are  $\dot{\theta}_2(0) = -\dot{\theta}_3(0) = 1$  and  $\dot{x}_0(0) = 1/3(\sin \alpha_2 - \sin \alpha_3)$  such that the linear and angular momenta of the cylinders, but not of the whole fluid-body system, are zero initially. The equilibrium positions on the ring are  $\alpha_1 = 0$ ,  $\alpha_2 = 19\pi/24$  and  $\alpha_3 = 29\pi/24$ . The non-dimensional parameters are  $\epsilon = 0.5$ ,  $k_1 = k_3 = 1$  and  $k_2 = 30$ .

This oscillation-induced rotation can be thought of as the rotational analogue of the dynamics discussed in Kanso & Newton (2009) for the rectilinear spring-mass system. To this end, analogously to the linear system, when exciting only the (symmetric) oscillatory mode  $\Gamma_3$  (impulsively or through deformation), both the net rotation mode  $\Gamma_1$  and the oscillatory mode  $\Gamma_2$  remain identically zero for all time. This response can be understood based on symmetry arguments, see Kanso & Newton (2009) for more details.

## 6.2. Free ring

Given that we now know that the fixed ring configuration is able to couple its oscillation nonlinearly with the surrounding fluid, we address the more interesting and complex question of how a system can exploit this angular momentum/energy exchange with the surrounding fluid in order to locomote. Thus, in the remainder of this paper we no longer fix the centre of the ring, but allow it to move freely in response to the net forces that act on it.

By way of judiciously chosen examples, starting with zero linear and angular momenta of the cylinders only, figure 5 depicts perhaps the simplest case (in the sense that it produces a rectilinear motion of the ring's centre) in which the ring is able to achieve net locomotion via coupling to the surrounding fluid, whereas the hydro-dynamically decoupled system and the rigidly locked system remain in place. Figures 6(a) and 6(b) show the trajectories of the centre of mass and the geometric centre of the ring, respectively, in comparison to those of the hydrodynamically decoupled system. Note that the rigidly locked system remains at rest for this set of initial conditions (initial conditions and parameters are given in the figure caption). We note that this is a highly specialized and perfect example in which no net rotation occurs due to oscillations, only translation. The more general (and interesting) case

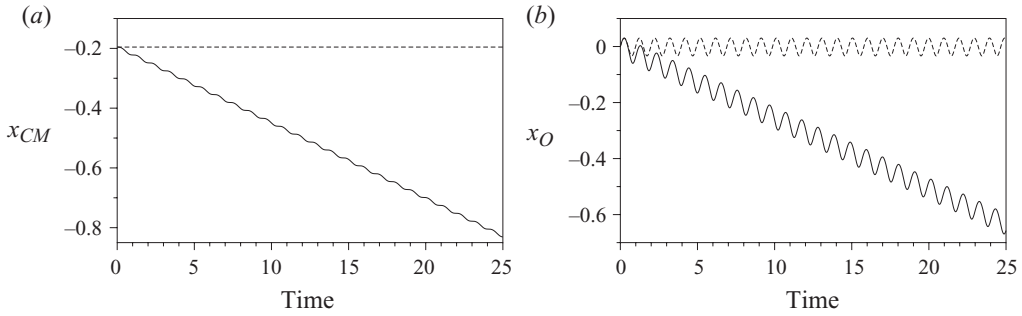


FIGURE 6. Submerged three-mass system on the free ring shown in figure 5. Continuous line – the trajectories of the fully coupled system, dashed line – the trajectories of the hydrodynamically decoupled system for (a) the centre of mass and (b) the geometric centre as functions of time. Clearly, the decoupled system undergoes no net motion. This is also true for the locked system which for this choice of initial conditions remains at rest for all time.

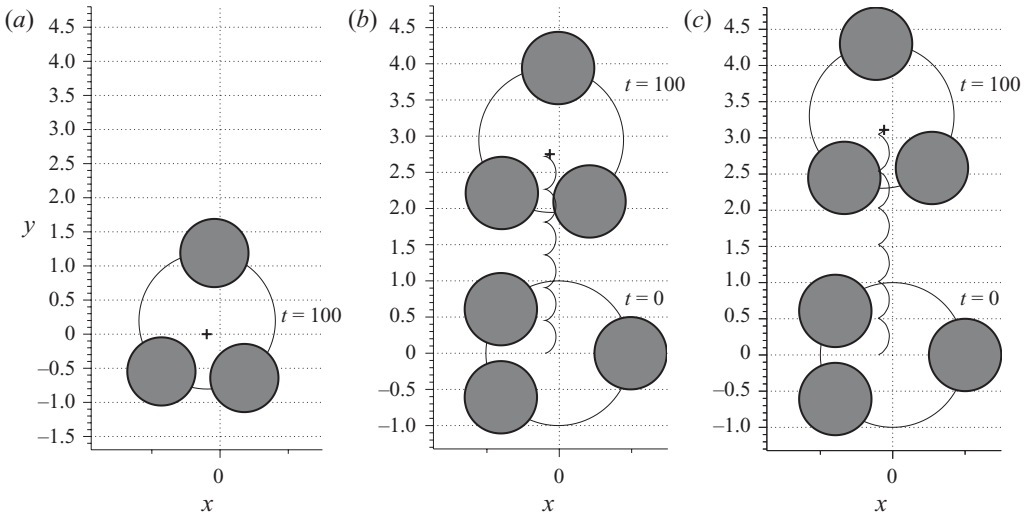


FIGURE 7. Rotation induces locomotion of the submerged free ring system. The non-zero initial conditions are  $\dot{\theta}_1(0) = 1$ ,  $\dot{\theta}_2(0) = \dot{\theta}_3(0) = \sec(5\pi/24)/2$  and correspond to an impulsive start for the masses from the equilibrium position such that the resulting linear momenta of the cylinders are zero initially. The non-dimensional parameters are the same as in figure 5. The configuration of the system and trajectory of the centre of mass at  $t = 100$  for (a) an elastic, hydrodynamically decoupled system, (b) a rigid body and (c) an elastic, fully coupled body. Clearly, the hydrodynamic effects couple the oscillations and rotation in a way that is advantageous to the net displacement of the ring.

is depicted in figure 7. Here, the initial conditions are such that the ring rotates as well as translates as it locomotes. The three panels of figure 7 contrast three important cases: (a) the elastic hydrodynamically decoupled system, (b) the trajectory of the corresponding rigid body and (c) the elastic, fully coupled system. Figure 8 shows the conserved quantities and the exchange of energy and momentum for the case shown in figure 7. Although the ring must use part of its energy for rotation

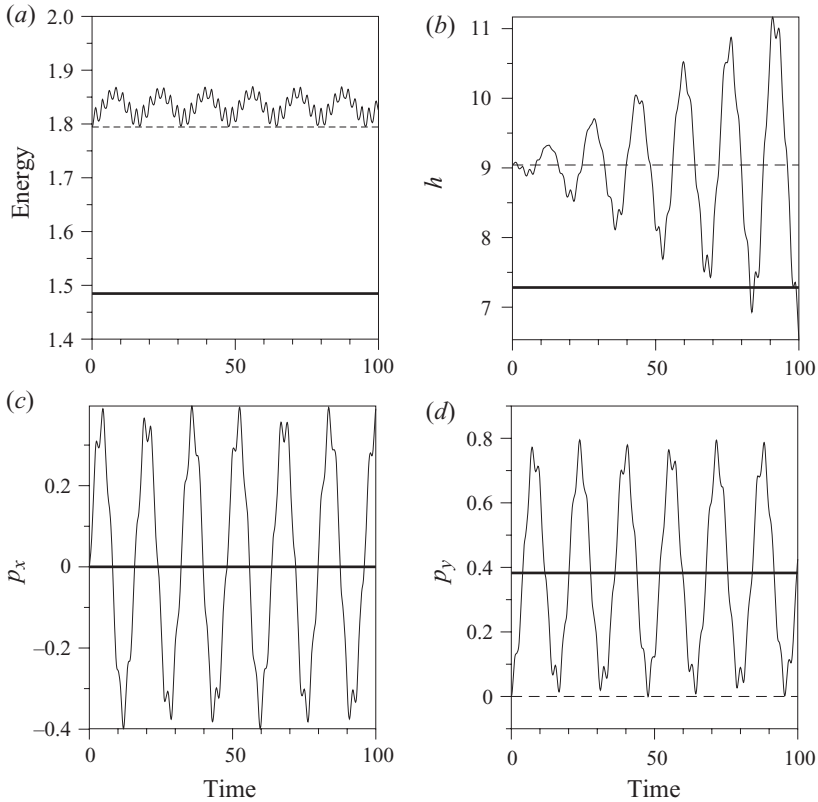


FIGURE 8. Conserved quantities for the case in figure 7. (a) Energy, (b) angular, (c) horizontal and (d) vertical momenta. Thick lines – quantities associated with the whole body–fluid system, thin continuous lines – quantities afferent to the cylinders only, and dashed lines – hydrodynamically decoupled system. Note that while the total energy and momenta of the body–fluid system are conserved (thick lines), there is an exchange of energy and momenta between the ring (thin lines) and the surrounding fluid.

(at the expense of translation), it gains by being able to locomote along a much more complex two-dimensional (curved) path, as most clearly depicted in figure 9. Here, figure 9(a) depicts the centre of mass of the locomoting ring, while 9(b) depicts the geometric centre with the same parameters as those chosen in figure 5. Our main point here is to depict the complex two-dimensional curved path that the system achieves.

In figure 10 we make a different point. Here we show a case in which the initial oscillations of the system, which has no angular momentum, induce rotation to the ring under coupling with the fluid. Thus, the trajectory in figure 10(a) is not along a straight line, but a curved path. This is most clearly seen by plotting the response of the system projected onto the rigid rotation mode as shown in figure 10(b).

In figures 11 and 12 we again make two separate points that highlight the differences between the ring if it is able to deform ( $k < \infty$ ) as opposed to a non-deformable (locked) body ( $k = \infty$ ). Figure 11 makes the point that there are initial conditions one can find such that the deformable body purely rotates, while the non-deformable body, with the same initial conditions, translates. Likewise, figure 12 shows that there are other initial conditions which make the deformable body

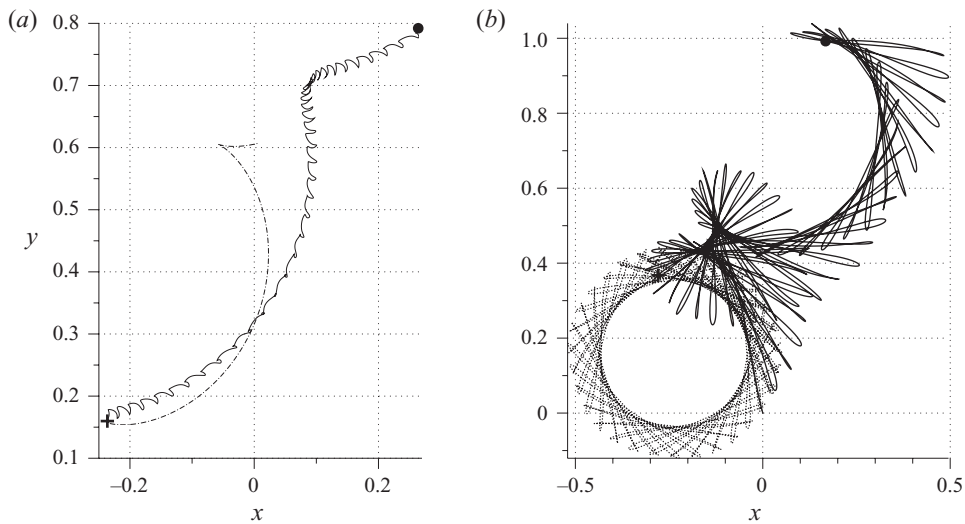


FIGURE 9. Trajectories of (a) the centre of mass: continuous line – the fully coupled system, dashed line – the rigidly locked system and (b) the geometric centre: continuous line – the fully coupled system, dashed line – the hydrodynamically decoupled system. The time interval is  $t = [0, 100]$ . The non-zero initial conditions are  $\Theta_1(0) = 1$ ,  $\dot{\Theta}_1(0) = 1/6$  and correspond to an impulsive start with initial deformation in the springs such that the linear momentum of the cylinders (without the fluid) is initially zero. The parameters are the same as in the case considered in figure 5.

translate, while the non-deformable body, for the same initial conditions, rotates in place.

## 7. Conclusions

The spring–mass ring that is free to move underwater due to its own deformations is a simple model for an underwater swimmer which locomotes by coupling its intrinsic body elasticity with the surrounding fluid, even in an inviscid, irrotational context. Through a series of increasingly complex examples, we highlight the following main points.

(i) The surrounding fluid couples the normal modes of oscillation of the spring–mass system and provides an environment in which the oscillator can exchange energy and angular momentum with the fluid to accomplish various modes of locomotion.

(ii) Viscous boundary conditions and the resulting generation of vorticity from the boundary layer region are not required for non-trivial energy and angular momentum exchange to occur.

(iii) Elasticity of the body (finite  $k$ ) (in the form of oscillations in our model) can sometimes be the essential ingredient for locomotion and turning manoeuvres, the details of which all depend on features such as phasing of the oscillations, their amplitudes and frequencies.

Of course all of these features will also play a role in the viscous case where a boundary layer is created and vorticity is shed into the wake region in response to different deformations. Indeed the next step in the long-term development of this class of models is to include wake dynamics and implement control strategies to produce more complex manoeuvres, such as turning and fleeing responses, collision avoidance



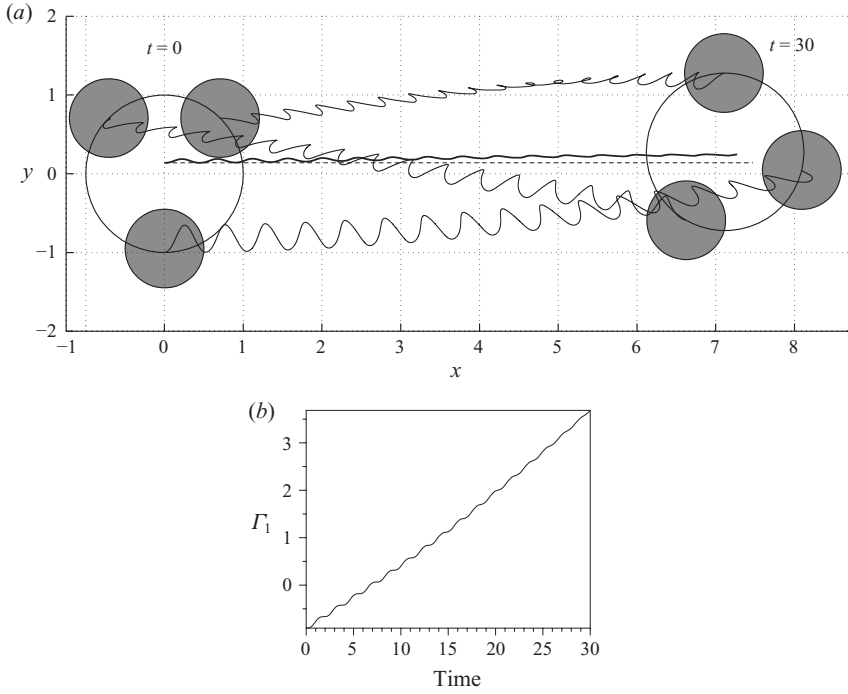


FIGURE 10. Passive oscillations induce rotation. (a) The configurations of the system at  $t=0$  and  $t=30$  are superimposed on the trajectory of the centre of mass (continuous line). The dashed line corresponds to the trajectory of the centre of mass of the locked system (no elasticity). The non-zero initial conditions are  $\dot{x}_O(0)=0.5$  and  $\Theta_2(0)=-\pi/6$ ,  $\Theta_3(0)=-\pi/12$  and correspond to an impulsive start in the horizontal direction and an initial configuration that is symmetric with respect to the  $x$ - and  $y$ -directions. The non-dimensional parameters are  $\epsilon=0.5$ ,  $k=2$ , and the cylinders are equally spaced on the ring at equilibrium. (b) The response of the system projected on the rigid rotation mode  $\Gamma_1 = (\Theta_1 + \Theta_2 + \Theta_3)/\sqrt{3}$ .

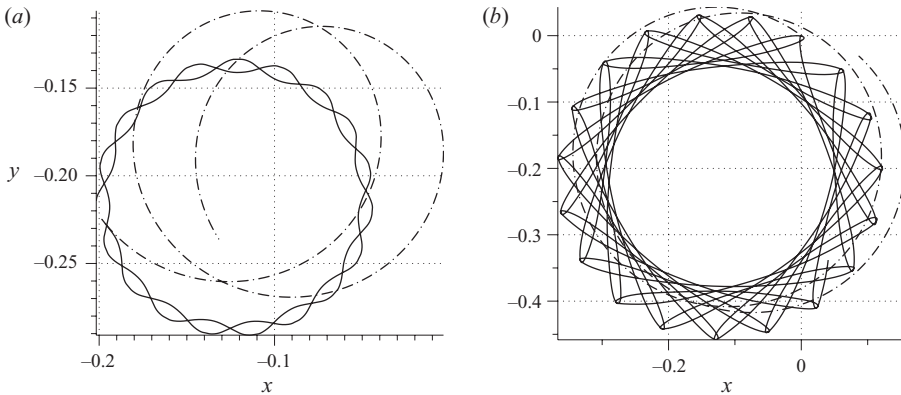


FIGURE 11. Deformable body rotates in place while the locked body under the same initial conditions translates as well as rotates. The trajectories of (a) the centre of mass and (b) the geometric centre are shown in dimensional coordinates. Continuous lines – the elastic, fully coupled system and dashed lines – the rigidly locked system. The non-zero initial conditions are  $\Theta_2(0)=\Theta_3(0)=1$ ,  $\dot{x}_O(0)=-0.03$ ,  $\dot{\Theta}_1(0)=0.3$ ,  $\dot{\Theta}_2(0)=0.233$ ,  $\dot{\Theta}_3(0)=0.198$ , and correspond to the total (fluid + body) linear momentum being zero and a non-zero angular momentum. The integration time is 123. The non-dimensional parameters are  $a=1$ ,  $\epsilon=0.4$ ,  $\delta=\pi/6$ ,  $k_1=k_3=0.1$ ,  $k_2=30$ .

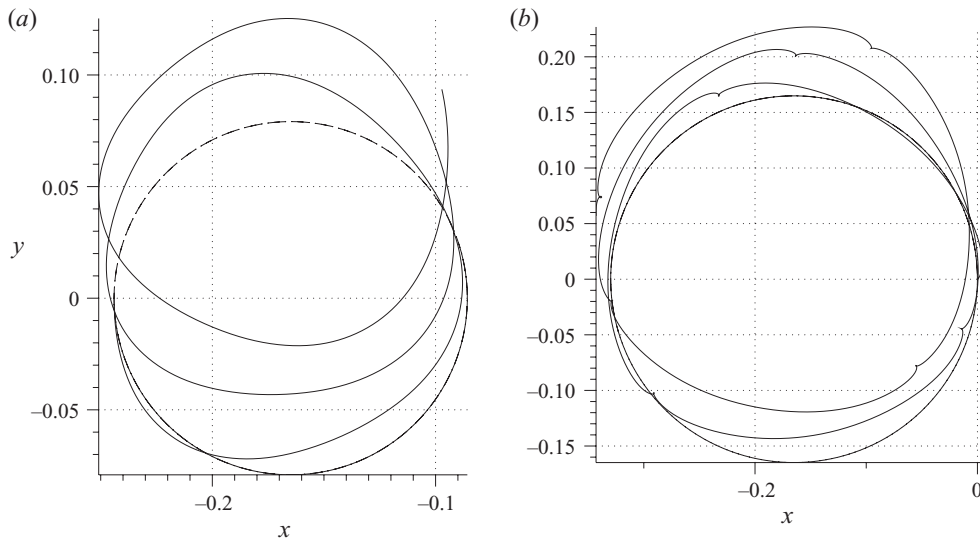


FIGURE 12. Deformable body translates while the locked body under the same initial conditions rotates in place. The trajectories of (a) the centre of mass and (b) the geometric centre are shown in dimensional coordinates. Continuous lines – the elastic, fully coupled system and dashed lines – the rigidly locked system. The non-zero initial conditions are  $\dot{\theta}_1(0) = 1.209$  and  $\dot{\theta}_2(0) = \dot{\theta}_3(0) = 0.835$ , and correspond to the total (fluid + body) linear momentum being zero and a non-zero angular momentum. The integration time is 40. The non-dimensional parameters are the same as in figure 11.

in the presence of more than one locomotor, multi-body synchronization, and general motion planning.

This work is partially supported by the National Science Foundation through the CAREER award CMMI 06-44925, the Grant CCF 08-11480 (RT and EK) and the Grant NSF-DMS-0804629 (RT and PKN).

#### REFERENCES

- BEAL, D. N., HOVER, F. S., TRIANTAFYLLOU, M. S., LIAO, J. C. & LAUDER, G. V. 2006 Passive propulsion in vortex wakes. *J. Fluid Mech.* **549**, 385–402.
- BRENNEN, C. E. 1982 A review of added mass and fluid inertial forces, *Tech. Rep.* CR 82.010. Naval Civil Engineering Laboratory, N62583-81-MR-554.
- BURTON, D. A., GRATUS, J. & TUCKER, R. W. 2004 Hydrodynamic forces on two moving disks. *Theor. Appl. Mech.* **31**, 153–188.
- CROWDY, D. G., SURANA, A. & YICK, K.-Y. 2007 The irrotational flow generated by two planar stirrers in inviscid fluid. *Phys. Fluids* **19**, 018103.
- GROTTA RAGAZZO, C. 2002 Dynamics of many bodies in a liquid: added-mass tensor of compounded bodies and systems with a fast oscillating body. *Phys. Fluids* **14** (5), 1590–1601.
- GROTTA RAGAZZO, C. 2003 On the motion of solids through an ideal liquid: approximated equations for many body systems. *SIAM J. Appl. Math.* **63** (6), 1972–1997.
- KANSO, E., MARSDEN, J. E., ROWLEY, C. W. & MELLI-HUBER, J. 2005 Locomotion of articulated bodies in a perfect fluid. *J. Nonlinear Sci.* **15**, 255–289.
- KANSO, E. & NEWTON, P. K. 2009 Passive locomotion via normal-mode coupling in a submerged spring–mass system. *J. Fluid Mech.* **641**, 205–215.
- LAMB, H. 1932 *Hydrodynamics*, 6th edn. Dover.

- LONG, H. J. & NIPPER, K. S. 1996 The importance of body stiffness in undulatory propulsion. *Am. Zool.* **36**, 678–694.
- LONG, J., HALE, M., MCHENRY, M. & WESTNEAT, M. 1996 Functions of fish skin: flexural stiffness and steady swimming of longnose gar, *Lepisosteus osseus*. *J. Exp. Biol.* **199**, 2139–2051.
- NAIR, S. & KANSO, E. 2007 Hydrodynamically-coupled rigid bodies. *J. Fluid Mech.* **592**, 393–411.
- VIDELER, J. J. 1993 *Fish Swimming*. Springer.
- VIDELER J. J. & WEIHS, D. 1982 Energetic advantages of burst-and-coast swimming of fish at high speeds. *J. Exp. Biol.* **97**, 169–178.
- WANG, Q. X. 2004 Interaction of two circular cylinders in inviscid fluid. *Phys. Fluids* **16**, 4412–4425.